Numerical analysis on the feasibility of a multi-layered dielectric sphere as a three-dimensional photonic crystal

Imakita, Kenji
Shibata, Hiroki
Fujii, Minoru
Hayashi, Shinji

(Citation)
Optics Express,21(9):10651-10658

(Issue Date)
2013

(Resource Type)
journal article

(Version)
Version of Record

(URL)
https://hdl.handle.net/20.500.14094/90002583

Numerical analysis on the feasibility of a multi-layered dielectric sphere as a three-dimensional photonic crystal

Kenji Imakita,* Hiroki Shibata, Minoru Fujii, and Shinji Hayashi

Department of Electrical and Electronic Engineering, Graduate School of Engineering, Kobe University, Rokkodai, Nada, Kobe 657-8501, Japan

imakita@eedept.kobe-u.ac.jp

Abstract: The radiative decay rate of a dipole emitter inside the core of a multi-layered dielectric sphere is theoretically investigated. It is shown that, when the thickness of each layer coincides with a quarter wavelength, the multi-layered sphere has a great potential to work as a three-dimensional photonic crystal with a high quality factor and a small mode volume. From the analysis of the dipole position dependence of a radiative decay rate, we show that a smaller core radius, a quarter wavelength at the smallest, is more suitable for real applications. The investigation on the tolerance for thickness nonuniformity reveals that the thickness variation of 10% is tolerable.

OCIS codes: (160.5293) Photonic bandgap materials; (160.5298) Photonic crystals; (160.1245) Artificially engineered materials.

References and links

1. S. Noda, M. Fujita, and T. Asano, "Spontaneous-emission control by photonic crystals and nanocavities," Nat. Photonics **1**, 449–458 (2007).
2. P. Lodahl, A. F. Van Driel, I. S. Nikolaev, A. Irman, K. Overgaag, D. Vanmaekelbergh, and W. L. Vos, "Controlling the dynamics of spontaneous emission from quantum dots by photonic crystals," Nature **430**, 654–657 (2004).
3. A. Tandaechanurat, S. Ishida, D. Guimard, M. Nomura, S. Iwamoto, and Y. Arakawa, "Lasing oscillation in a three-dimensional photonic crystal nanocavity with a complete bandgap," Nat. Photonics **5**, 91–94 (2011).
4. L. A. Stewart, Y. Zhai, J.M.Dawes, M. J. Steel, J. R.Rabeau, M. J. Withford, "Single photon emission from diamond nanocrystals in an opal photonic crystal," Opt. Express **17**, 18044–18053 (2009).
5. G. Burlak, S. Koshevaya, J. Sanchez-mondragon, and V. Grimalsky, "Electromagnetic eigenoscillations and fields in a dielectric microsphere with multilayer spherical stack," Opt. Commun. **187**, 91–105 (2001).
6. Z. Ren, T. Zhai, Z. Wang, J. Zhou, and D. Liu, "Complete band gaps in the visible range achieved by low-refractive-index material," Adv. Mater. **20**, 2337–2340 (2008).
7. D. Sharp, A. Turberfield, and R. Denning, "Holographic photonic crystals with diamond symmetry," Phys. Rev. B **68**, 205102 (2003).
8. D. K. Yi, S. S. Lee, G. C. Papaefthymiou, and J. Y. Ying, "Nanoparticle architectures templated by SiO_2/Fe2O_3 nanocomposites," Chem. Mater. **18**, 614–619 (2006).
9. H.-W. Kwon, Y.-M. Lim, S. K. Tripathy, B.-G. Kim, M.-S. Lee, and Y.-T. Yu, "Synthesis of Au/TiO_2 core-shell nanoparticles from titanium isopropoxide and thermal resistance effect of TiO_2 shell," Jpn. J. Appl. Phys. **46**, 2567–2570 (2007).
10. G.-C. Chen, C.-Y. Kuo, and S.-Y. Lu, "A general process for preparation of core-shell particles of general process for preparation of core-shell particles of complete and smooth shells," J. Am. Ceram. Soc. **88**, 277–283 (2005).
11. W. Liu, W. Zhong, H. Jiang, N. Tang, X. Wu, and Y. Du, "Highly stable alumina-coated iron nanocomposites synthesized by wet chemistry method," Surf. and Coat. Tech. **200**, 5170–5174 (2006).
12. H. Wang, M. Yu, C. Lin, X. Liu, and J. Lin, "Synthesis and luminescence properties of monodisperse spherical Y_2O_3:Eu^{3+}@SiO_2 particles with core-shell structure," J. Phys. Chem. C **111**, 11223–11230 (2007).

#186007 - $15.00 USD Received 26 Feb 2013; revised 4 Apr 2013; accepted 15 Apr 2013; published 24 Apr 2013

13. M. Lessard-viger, M. Rioux, L. Rainville. and D. Boudreau, "FRET enhancement in multilayer core-shell nanoparticles," Nano Lett. **9**, 3066–3071 (2009).
14. D. Brady, G. Papen, and J.E. Sipe, "Spherical distributed dielectric resonators," J. Opt. Soc. Am. B **10**, 646–657 (1993).
15. G. Sullivan and D.G. Hall, Radiation in spherically symmetric structures. II. "Enhancement and inhibition of dipole radiation in a spherical Bragg cavity," Phys. Rev. A **50**, 2708 (1994).
16. A. Moroz, "A recursive transfer-matrix solution for a dipole radiating inside and outside a stratified sphere," Ann. Phys. **315**, 352–418 (2005).
17. A. Moroz, "Spectroscopic properties of a two-level atom interacting with a complex spherical nanoshell," Chem. Phys. **317**, 1–15 (2005).
18. R. S. Meltzer, S. P. Feofilov, B. Tissue, and H. B. Yuan, "Dependence of fluorescence lifetimes of Y_2O_3:Eu^{3+} nanoparticles on the surrounding medium," Phys. Rev. B **60**, 14012–14015 (1999).
19. C. M. Herzinger, B. Johs, W. A. McGahan, J. A. Woollam, and W. Paulson, "Ellipsometric determination of optical constants for silicon and thermally grown silicon dioxide via a multi-sample, multi-wavelength, multi-angle investigation," J. Appl. Phys. **83**, 3323–3336 (1998).
20. V. Puri, "Refractive index and adhesion of Al_2O_3 thin films obtained from different processes - a comparative study," Thin Solid Films **288**, 120–124 (1996).
21. D.-J. Won, C.-H. Wang, H.-K. Jang, D.-J. Choi, "Effects of thermally induced anatase-to-rutile phase transition in MOCVD-grown TiO_2 films on structural and optical properties," Appl. Phys. A **73**, 595–600 (2001).
22. I. Abram, I. Rovert, and R. Kuszelwicz, "Spontaneous emission control in semiconductor microcavities with metallic or Bragg mirrors," IEEE J. Quantum Electron. **34**, 71–76 (1998).
23. K. Srinivasan, P. E. Barclay, O. Painter, J. Chen, A. Y. Cho, and C. Gmachl, "Experimental demonstration of a high quality factor photonic crystal microcavity," Appl. Phys. Lett. **83**, 1915–1917 (2003).
24. J. Li, X. Li, X. Sun, and T. Ishigaki, "Monodispersed colloidal spheres for uniform Y_2O_3:Eu^{3+} red-phosphor particles and greatly enhanced luminescence by simultaneous Gd^{3+} doping," J. Phys. Chem. C **112**, 11707–11716 (2008).
25. B. Aiken, W. P. HSU, E. Matijevic, "Preparation and properties of monodispersed colloidal particles of lanthanide compounds: III, Yttrium (III) and mixed yttrium (III)/cerium (III) systems," J. Am. Ceram. Soc. **71**, 845–853 (1988).
26. F. Wang, R. Deng, J. Wang, Q. Wang, Y. Han, H. Zhu, X. Chen, and X. Liu, "Tuning upconversion through energy migration in core-shell nanoparticles", Nat. Mater. **10**, 968–973 (2011).

1. Introduction

A three-dimensional photonic crystal is an artificially engineered periodic dielectric material that exhibits bands and gaps in the photonic density of states [1–4]. The unique property of the photonic bandgap, i.e., the prohibition on the propagation of electromagnetic waves for all wavevectors, enables to control light with amazing facility and produce effects that are impossible with conventional optics. For example, by introducing artificial defect and/or light-emitters inside the photonic bandgap material, various scientific and engineering applications, such as control of spontaneous emission [1, 2], thresholdlless lasers [3], and single photon source [4] can be realized.

A multi-layered sphere, consisting of a core sphere covered by concentric spherical dielectric layers (spherical stack), is a class of a three-dimensional photonic crystal. When the optical thickness of each layer coincides with a quarter wavelength, the stack works as a Bragg mirror and can confine photons three-dimensionally inside the core sphere. The multi-layered sphere potentially has much higher quality factors (Q) compared to a bare microsphere because the stack permits the modes with stronger radial oscillation [5]. Due to the complete point symmetry about the center of the sphere, the photonic density of states inside the core can be designed with higher flexibility than in other conventional photonic crystals. In fact, a complete photonic band gap in the visible region can be realized in a multi-layered sphere with refractive index contrast in the stack as low as 0.15 [6], which is one order of magnitude smaller than that required for the conventional photonic crystals with a diamond structure [7].

Experimentally, due to a rapid progress in the field of nano technology, there have been numerous reports on the coating of dielectric spherical layers on the surface of nanoparticles by chemical solution processes [8–13]. However, so far, the thickness of each layer has not

#186007 - $15.00 USD Received 26 Feb 2013; revised 4 Apr 2013; accepted 15 Apr 2013; published 24 Apr 2013

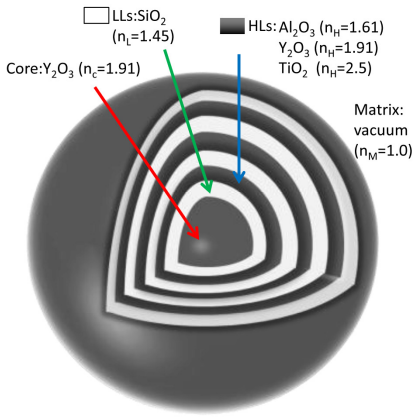

Fig. 1. A schematic of a multi-layered sphere.

been carefully controlled so that the modification of the photonic mode density of states could not be achieved. Theoretically, in 1993, Brady et al. [14] studied electromagnetic modes inside a multi-layered sphere without a radiating dipole. In 1994, Sullivan et al. [15] calculated the radiative decay rate of a radiating dipole placed at the center of a multi-layered sphere. In 2005, Moroz [16] presented a general solution for the radiative decay rate of a radiating dipole placed in an arbitrary position in a multi-layered sphere. The algorithm has no limitation on the dipole position, the number of layers, the layer thickness and the layer medium. By employing the algorithm, he calculated the radiative decay rate of a dipole placed in a three- or four-layered sphere consisting of metal and dielectric layers [16, 17]

In this work, we apply the algorithm to a multi-layered sphere, consisting of quarter-wave dielectric concentric layers. We show that it has a great potential to work as a three-dimensional photonic crystal with a high Q and a small mode volume (V). In addition, we study the tolerance for the position of the dipoles and the variation of the layer thickness to achieve the high performance. We demonstrate that the tolerance is large enough to be realized by using the state of the art chemical synthesis technology.

2. Calculation procedure

A normalized radiative decay rate, which is defined as a radiative decay rate of a dipole emitter inside the multi-layered sphere with respect to that in the free-space medium, can be calculated by a procedure described in Ref. [16]. First, a dipole is placed in the core of multi-layered sphere and the electric and magnetic fields were calculated by a recursive transfer method. Then the time-averaged total radiated power (radiative loss) was calculated by integrating the time-averaged Poynting vector over the surface of a sphere with an infinite radius. The ratio of the calculated radiative loss to that of a dipole placed in a free space results in the normalized radiative decay rate (Eq. 126 in Ref. [16]). In the case that the dipole is placed off the center of the sphere, the normalized radiative decay rate depends on the orientation of the dipole. The orientation average of the normalized radiative decay rate (Γ/Γ_0) was calculated by $\Gamma/\Gamma_0 = 1/3\Gamma_\perp/\Gamma_0 + 2/3\Gamma_\parallel/\Gamma_0$, where $\Gamma_\perp/\Gamma_0$ and $\Gamma_\parallel/\Gamma_0$ are the normalized radiative decay rate of the radially- and tangentially-oriented dipoles. Note that Γ/Γ_0 corresponds to the well-known

#186007 - $15.00 USD Received 26 Feb 2013; revised 4 Apr 2013; accepted 15 Apr 2013; published 24 Apr 2013

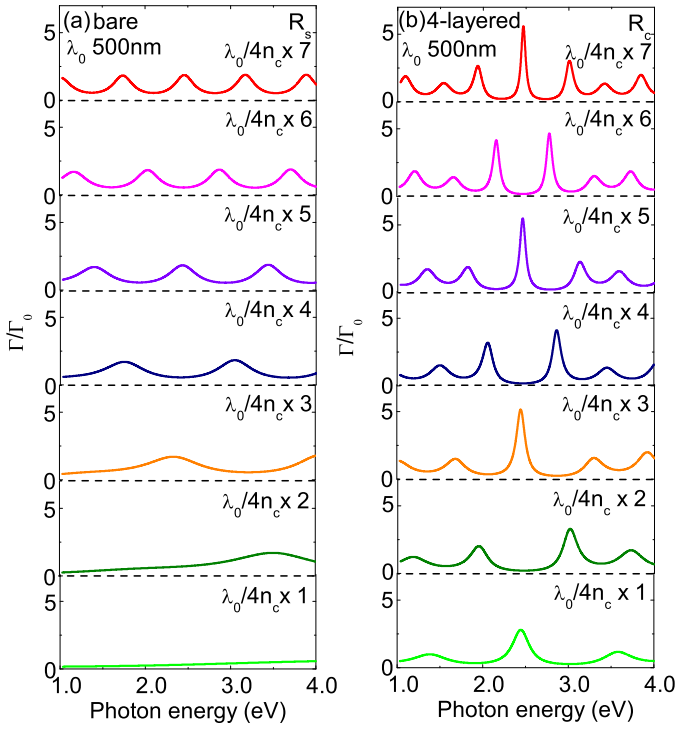

Fig. 2. Core radius dependence of Γ/Γ_0 spectra of a dipole inside the core of (a) a bare sphere and (b) a 4-layered sphere.

Purcell factor.

3. Results and discussion

Figure 1 shows a schematic of a multi-layered sphere. It consists of a core covered by concentric spherical dielectric layers. In this work, the refractive index of the core (n_c) is fixed to 1.91, which corresponds to that of yttrium oxide (Y_2O_3) [18]. The spherical dielectric layers consist of alternate high- and low-index layers (HLs and LLs). The first layer on the surface of the core is a LL. The refractive index of LLs (n_L) is fixed to 1.45, which is equal to that of silicon dioxide (SiO_2) [19]. The refractive indices of HLs (n_H) are 1.61, 1.91 or 2.50, which corresponds to those of aluminum oxide (Al_2O_3), Y_2O_3, and titanium dioxide (TiO_2), respectively [18,20,21]. The thickness of each layer is a quarter optical wavelength ($\lambda_0/4n_H$ or $\lambda_0/4n_L$), where λ_0 is designed to be 500 nm. The refractive index of surrounding matrix (n_M) is 1.0, assuming that the sphere is in vacuum. Note that all these materials can be synthesized by chemical solution processes [8–12].

Figure 2(a) shows the normalized radiative decay rate of a dipole inside a bare sphere. The sphere radius (R_s) is varied from $\lambda_0/4n_c$ to $7\lambda_0/4n_c$. We can see that the normalized radiative decay rate have some peaks, arising from resonances to so called whispering gallery modes. The number of the peaks increases with increasing R_s, while the peak intensity is independent of R_s. Figure 2(b) shows the normalized radiative decay rate of a dipole placed at the center of

#186007 - $15.00 USD Received 26 Feb 2013; revised 4 Apr 2013; accepted 15 Apr 2013; published 24 Apr 2013

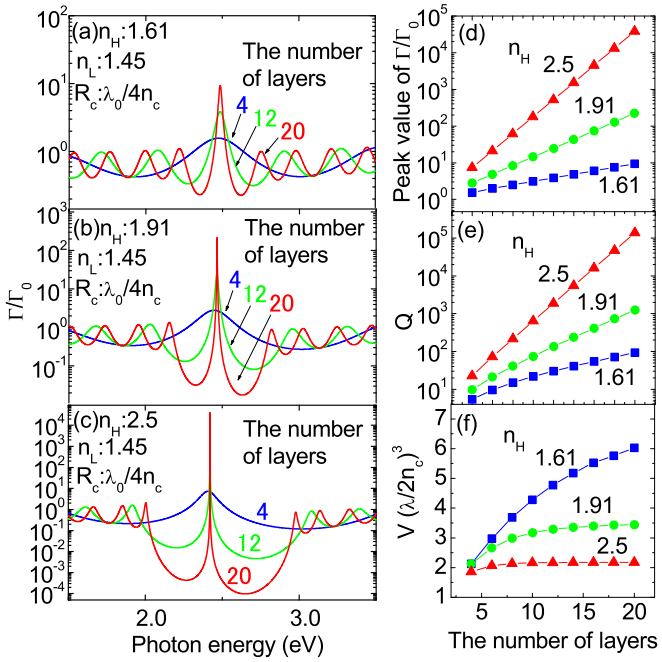

Fig. 3. (a-c) Dependence of Γ/Γ_0 spectra on the number of layers. n_H are chosen to be (a)1.61, (b)1.91, and (c)2.50, respectively. (d) Peak value of Γ/Γ_0, (e)Q, and (f)V, as a function of the number of layers.

the core coated by 4 layers (2 HLs and 2 LLs). n_H is 1.91. The core radius (R_c) is the same as R_s in Fig. 2(a). We can see that when R_c equals to $(2n+1)\lambda_0/4n_c$ (n : *integer*), the normalized radiative decay rate is the largest at λ_0 (2.48 eV in energy), while it is suppressed around λ_0 when R_c coincides with $2n\lambda_0/4n_c$. This result is qualitatively similar to the case of an one-dimensional Bragg resonator [22]. In the case of R_c of $(2n+1)\lambda_0/4n_c$, the peak value of the normalized radiative decay rate of a dipole placed in a 4-layered sphere is twice larger than that of a dipole placed in a bare sphere. The coating of only 4 layers has a significant effect on the noramalized radiative decay rate.

Figure 3(a) shows the dependence of the normalized radiative decay rate on the number of layers. n_H and R_c are 1.61 and $\lambda_0/4n_c$, respectively. We can see that the peak value of the normalized radiative decay rate at λ_0 increases with increasing the number of layers. When the number of layers is 20, it reaches about 10. In Figs. 3(b) and 3(c), n_H are changed to 1.91 and 2.50, respectively. The normalized radiative decay rate is larger for larger n_H. In Fig. 3(c), the normalized radiative decay rate becomes as high as 40000 at the resonant peak, when the number of layers is 20. In addition, beside the resonant peak, we can see a region where the normalized radiative decay rate is suppressed to as low as 0.0001. The suppression region corresponds to a so called photonic band gap. The size of the band gap, which is defined as the energy difference between the upper and lower band, is as large as 0.9 eV with the center of 2.48 eV. In Fig. 3(d), the peak value of the normalized radiative decay rate is plotted as a function of the number of layers. It grows exponentially with increasing the number of layers and/or n_H. The Q and V of the multi-layered sphere are plotted in Figs. 3(e) and 3(f). Q is

#186007 - $15.00 USD Received 26 Feb 2013; revised 4 Apr 2013; accepted 15 Apr 2013; published 24 Apr 2013

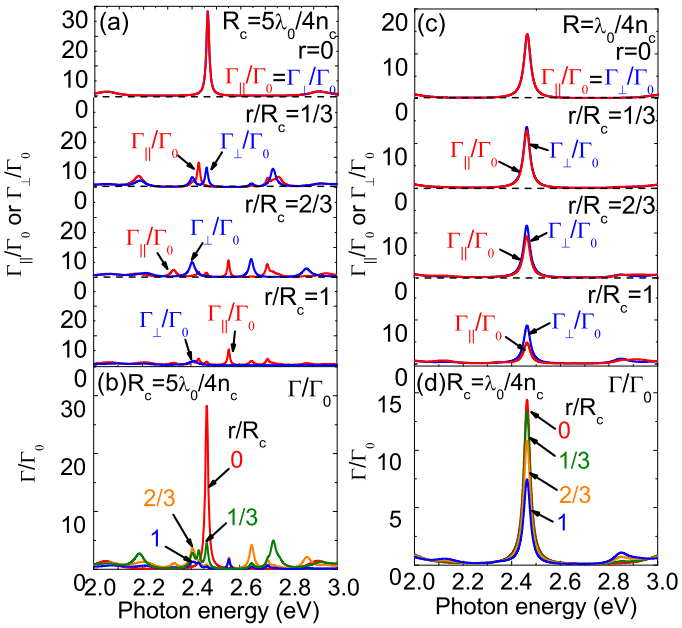

Fig. 4. Normalized radiative decay rate spectra as a function of the position of the dipole (r). R_c is (a,b)$5\lambda/4n_c$ and (c,d)$\lambda_0/4n_c$, respectively.

obtained by $\omega_0/\Delta\omega$ where ω_0 and $\Delta\omega$ are the resonant frequency and the full width at half maximum of the normalized radiative decay rate spectrum. V is obtained from the following relation [23]

$$\frac{\Gamma}{\Gamma_0} = \frac{3Q(\frac{\lambda}{n_c})^3}{4\pi^2 V} \tag{1}$$

where λ is the mode's wavelength. Similar to the normalized radiative decay rate, Q shows exponential dependence on the number of layers. On the other hand, V tends to saturate when the number of layers increases. The higher n_H causes the saturation at smaller number of layers. At the saturation region, V is smaller for higher n_H because higher index contrast can confine electromagnetic fields more strongly. It reaches $2.1(\lambda/2n_c)^3$ for the n_H of 2.5. These results suggest that the multi-layered sphere has a great potential working as a three-dimensional photonic crystal with a high Q and a small V.

Figure 4(a) shows $\Gamma_\perp/\Gamma_0$ and $\Gamma_\parallel/\Gamma_0$ spectra as a function of the position of the dipole (r) with respect to R_c. n_H and R_c are 1.91 and $5\lambda/4n_c$ respectively. The number of layers is 15. When $r/R_c = 0$, $\Gamma_\perp/\Gamma_0$ and $\Gamma_\parallel/\Gamma_0$ spectra are identical. With increasing r/R_c, the shape of the $\Gamma_\perp/\Gamma_0$ and $\Gamma_\parallel/\Gamma_0$ spectra becomes different, due to the coupling with different modes inside the multi-layered sphere. Figure 4(b) demonstrates Γ/Γ_0 as a function of r/R_c. When the dipole is located at the surface of the core sphere ($r/R_c = 1$), the peak value of the Γ/Γ_0 is one order of magnitude smaller than that of the case of the dipole located at the center ($r/R_c = 0$). This implies that, when R_c is $5\lambda/4n_c$, the control of the emitter position in the core sphere is indispensable for the real application. With decreasing R_c, the position dependence of the normalized radiative decay rate becomes smaller. Figure 4(c) shows the results for the R_c

#186007 - $15.00 USD Received 26 Feb 2013; revised 4 Apr 2013; accepted 15 Apr 2013; published 24 Apr 2013

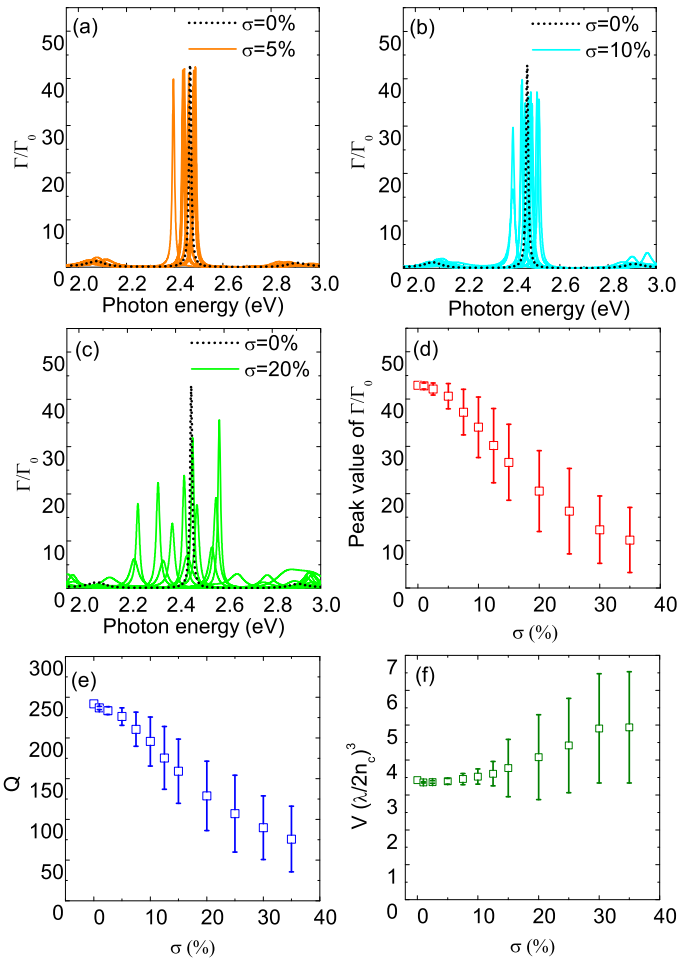

Fig. 5. Γ/Γ_0 spectra as a function of σ of layer thickness distributions. σ is (a)5%, (b)10%, and (c)20%, with respect to a quarter optical wavelength. (d)Peak value of Γ/Γ_0, (e)Q, and (f)V as a function of σ.

of $\lambda/4n_c$. We can see that $\Gamma_\perp/\Gamma_0$ and $\Gamma_\parallel/\Gamma_0$ spectra have the same peak energy and no other peaks appear for any r from 0 to R_c. This small dipole position dependence is due to the absence of other electromagnetic modes which can be coupled with the dipole because of the small core radius. In Fig. 4(d), Γ/Γ_0 is plotted as a function of r. The peak value of the Γ/Γ_0 decreases only 50% with increasing r. This decrease is much smaller than the case of R_c of $5\lambda/4n_c$. In addition, when R_c is $\lambda/4n_c$, there are no peaks other than the main peak in the photonic band gap. These results suggest that fine control of the emitter position is not necessarily required when R_c is $\lambda/4n_c$. It should be noted here that $\lambda/4n_c$ is of the order of several tens nanometers when λ is in the visible region. The fabrication techniques of luminescent particles in this size range have been well established in the field of chemical synthesis of nanoparticles in a solution phase [24, 25].

#186007 - $15.00 USD Received 26 Feb 2013; revised 4 Apr 2013; accepted 15 Apr 2013; published 24 Apr 2013

Figure 5(a-c) shows the normalized radiative decay rate as a function of the standard deviation of the layer thickness (σ). n_H, R_c and the number of layers are 1.91, $\lambda/4n_c$, and 15, respectively. In Fig. 5(a), solid spectra are the calculation results of Γ/Γ_0 for 10 patterns of randomly-created thickness distributions with σ of 5% with respect to a quarter optical wavelength. The dotted spectrum is a result for σ of 0%. We can see no significant deterioration of the peak value of Γ/Γ_0 in the case of σ of 5%, although the peak positions fluctuate. Figures 5(b) and 5(c) are results for σ of 10% and 20%. With increasing σ, the normalized radiative decay rate spectra broaden and the peak value decreases. In Figs. 5(d), 5(e), and 5(f), the peak value of Γ/Γ_0, Q, and V, respectively, averaged over 100 patterns of thickness distributions are plotted as a function of σ. With increasing σ, the peak value of Γ/Γ_0 and Q decreases significantly, while V increases slightly. In order to keep the deterioration of Γ/Γ_0 smaller than 30% compared to the original value, σ should be less than 10% of a quarter wavelength. This requires thickness control with the accuracy of the order of nanometer. This seems feasible to achieve experimentally by the state of the art chemical synthesis technology [26].

4. Conclusion

In conclusion, the radiative decay rate of a dipole emitter inside the core of a multi-layered dielectric sphere has been theoretically investigated. It is shown that, when the thickness of each layer coincides with a quarter wavelength, the multi-layered sphere works as a photonic crystal with a high Q and a small V. The dipole position dependence of the radiative decay rate is found to be smaller for smaller core radius, suggesting that the core radius of a quarter optical wavelength, corresponding to several tens nanometers for visible wavelengths, is suitable for applications. It is also found that the thickness variation should be less than 10% to keep the deterioration of the radiative decay rate less than 30%. These results suggest that a chemical synthesis in a solution phase is a feasible fabrication method of the multi-layered sphere as a three-dimensional photonic crystal.

#186007 - $15.00 USD Received 26 Feb 2013; revised 4 Apr 2013; accepted 15 Apr 2013; published 24 Apr 2013